Reusable surface confined semi-conducting metal-TCNQ and metal-$TCNQF_4$ catalysts for electron transfer reactions†

Manika Mahajan[a,b], Suresh K. Bhargava[a,b] and Anthony P. O'Mullane*[a]

The synthesis of organic semiconducting materials based on silver and copper-TCNQ (TCNQ = 7,7,8,8-tetracyanoquinodimethane) and their fluorinated analogues has received a significant amount of attention due to their potential use in organic electronic applications. However there is a scarcity in the identification of different applications for which these interesting materials may be suitable candidates. In this work we address this by investigating the catalytic properties of such materials for the electron transfer reaction between ferricyanide and thiosulphate ions in aqueous solution which to date has been almost solely limited to metallic nanomaterials. Significantly it was found that all the materials investigated, namely CuTCNQ, AgTCNQ, $CuTCNQF_4$ and $AgTCNQF_4$ were catalytically active and interestingly the fluorinated analogues were superior. $AgTCNQF_4$ demonstrated the highest activity and was tested for its stability and re-usability for up to 50 cycles without degradation in performance. The catalytic reaction was monitored via UV-visible and open circuit potential versus time measurements as well as an investigation of the transport properties of the films via electrochemical impedance spectroscopy. It is suggested that morphology and bulk conductivity are not the limiting factors but rather the balance between the accumulated surface charge from electron injection via thiosulphate ions on the catalyst surface and transfer to the ferricyanide ions which controls the reaction rate. The facile fabrication of these types of re-usable surface confined organic materials as catalytically active materials may have important uses for many more electron transfer reactions.

1. Introduction

The fabrication and characterisation of semi-conducting metal-TCNQ (TCNQ = 7,7,8,8-tetracyanoquinodimethane) has received significant interest since the discovery that the silver and copper based moieties demonstrate switching and field emission properties.[1-11] Although there have been numerous reports on methods of synthesis including chemical,[12-13] physical,[2, 9, 11] and recently electrochemical[3, 7, 14-17] and photochemical approaches,[18-19] the application of these materials is solely limited to molecular electronics, field emission and magnetic properties. Even derivatives of MTCNQ (M = Cu and Ag) such as $TCNQF_4$ and TCNAQ have only been investigated for these types of applications.[12, 20-21] However, the fluorinated analogues have received renewed interest from both a synthetic and application viewpoint[12, 22-25] where it was found that tuning the morphology of $CuTCNQF_4$ and $AgTCNQF_4$ had a significant impact on their field emission properties.[22] Even with well established synthesis routes and structural characterisation there are only four reports on different uses of this type of material to the best of our knowledge, i.e. CuTCNQ as a source/drain contact material in pentacene organic field effect transistors,[26] CuTCNQ decorated with gold nanoparticles as a photocatalyst,[27-28] $Zn(TCNQ)_2$ being used as a moisture sensing compound[29] and the photo-oxidation of water during the course of AgTCNQ photocrystallisation in an ionic liquid.[18] There are numerous advantages in investigating this type of material as synthesis is straightforward and properties such as conductivity can be controlled systematically by either changing the metal cation or the electron acceptor. The bonding arrangement between the central cation and the anions can also be varied, with the CuTCNQ case being of particular interest, as it can exist as both a kinetically and thermodynamically stable phase with significantly different conductivities.[13] This is due to differences in the stacking arrangement of the interpenetrating networks of TCNQ within the structures where phase I shows efficient π-stacking, and hence higher conductivity, compared to phase II which does not due to the larger distance between the individual TCNQ layers[13]. Given their facile fabrication and interesting electronic and structural properties it is surprising that these materials have not found more widespread use. This is now addressed whereby AgTCNQ, CuTCNQ phase I and phase II and their fluorinated analogues $AgTCNQF_4$ and $CuTCNQF_4$ are shown for the first time to act as catalysts for redox reactions. Significantly, the incorporation of the $TCNQF_4$ acceptor results in a dramatic increase in catalytic activity for the model electron transfer reaction in aqueous solution between potassium ferricyanide and sodium thiosulphate which results in a recoverable catalyst that is reusable for up to 50 cycles.

2. Experimental

Materials and chemicals: Silver and copper metal foils (99.99 % purity) were obtained from Chem Supply. 7,7,8,8-Tetracyanoquinodimethane (TCNQ), 2,3,5,6-tetrafluoro-7,7,8,8-tetracyanoquinodimethane ($TCNQF_4$) (Sigma), potassium ferricyanide (Ajax Finechem.), sodium thiosulphate (Merck) were used as received. TCNQ and $TCNQF_4$ solutions were prepared in acetonitrile (Aldrich). All aqueous solutions were prepared from water (resistivity of 18.2 MΩcm) purified by use of a Milli-Q reagent deioniser (Millipore).

MTCNQ and $MTCNQF_4$ formation Copper and silver foils (0.158 cm^2 area) were used to prepare the samples in this study. They were first immersed in HNO_3 (10% v/v) to remove any surface oxides and then washed with acetone and methanol followed by drying in a stream of nitrogen gas prior to modification. CuTCNQ phase I, AgTCNQ, and $CuTCNQF_4$ samples were prepared by immersing copper and silver foils in either 2 mM TCNQ or 1 mM $TCNQF_4$ solutions for 12 h. $AgTCNQF_4$ was prepared by placing silver foil in a de-gassed 1 mM $TCNQF_4$ solution. CuTCNQ phase II was prepared by immersing copper foil into a boiling acetonitrile solution that was saturated with TCNQ for 1 h. After all reactions, samples were rinsed briefly with acetonitrile and thoroughly with Milli-Q water and dried in a stream of nitrogen gas. For all experiments samples of geometric area 0.158 cm^2 were used.

Electrochemical measurements: Electrochemical experiments were conducted at (20 ± 2)°C with a CH Instruments (CHI 760C) electrochemical analyser. The working electrode was the sample of interest, the reference electrode was Ag/AgCl (aqueous 3M KCl) and a platinum wire was used as the counter electrode. EIS experiments were performed using a CH Instruments (CHI 920C) under quiescent conditions at the formal redox potential of 5 mM $Fe(CN)_6^{3-/4-}$ in 0.1 M NaCl at an amplitude of 10 mV over a frequency range of 0.01 – 10^6 Hz. The sample consisted of exposed MTCNQ or $MTCNQF_4$ material only and the copper or silver foil was masked using Kapton tape.

Catalytic reactions: The catalytic reactions (0.1 M thiosulphate and 1 mM potassium ferricyanide) at (20 ± 2)°C were analysed by UV-visible spectroscopy (Cary 50 Bio spectrophotometer) in a cell of 1 cm path length by taking aliquots from the 30 ml solution in which the sample was fixed under stirring conditions. A constant area was used for all samples and the stirring rate was maintained at 1200 rpm using a magnetic stirring bar at the bottom of the beaker. For the re-usability tests the experiments were performed in a 3 ml cuvette under stirring conditions (1200 rpm). Samples were washed thoroughly with Millipore water before each catalytic reaction was performed.

Surface characterisation: Surface characterisation was carried out using scanning electron microscopy (FEI Nova SEM), Fourier transform infrared spectroscopy (FT-IR Perkin-Elmer Spectrum 100), Raman spectroscopy (Perkin-Elmer Raman Station 200F) and XRD (Bruker D4 Endeavor – fitted with Lynxeye position sensitive detector). For XRD measurements the samples were mechanically removed from the surface.

3. Results and Discussion

A simple approach was taken for the synthesis of all materials whereby copper or silver foil was immersed in a solution of either TCNQ or $TCNQF_4$ in acetonitrile to generate the relevant material. This simple electron transfer reaction between the metal and solution based TCNQ has been used previously for CuTCNQ and AgTCNQ formation. Typical needle shaped rods are formed for both phase I CuTCNQ (Figure 1a) and AgTCNQ (Figure 1b) which are densely packed over the entire substrate as shown by the low magnification images in Figure S1. The needles in the case of AgTCNQ however are more isolated when compared to the bundles of needles seen for CuTCNQ. The fabrication of CuTCNQ phase II is achieved by heating the phase I film in a saturated solution of TCNQ in acetonitrile for 1 hr. The morphology subsequently changes showing a layered structure consisting of well packed sheets over the surface (Figure 1c).

This approach is also successful for the creation of the fluorinated analogues which to date has mostly been synthesised by chemical, electrochemical or physical vapour deposition methods. A distinct change in morphology occurs in comparison to the TCNQ based material with sharp interpenetrating plate like crystals observed for $CuTCNQF_4$ (Figure 1d) and thicker columnar rods for $AgTCNQF_4$ which are hollow in nature (Figure 1e). This type of morphology is unusual for the fluorinated analogues as typically nanowire like crystals are reported using the physical vapour deposition method which are applicable to field emission applications.[20] With the fabrication approach used here a homogeneous surface is also created for both fluorinated analogues as seen by the low magnification image in Figure S1. An added advantage of this protocol is that in principle very large areas of copper or silver substrates can be easily modified if required.

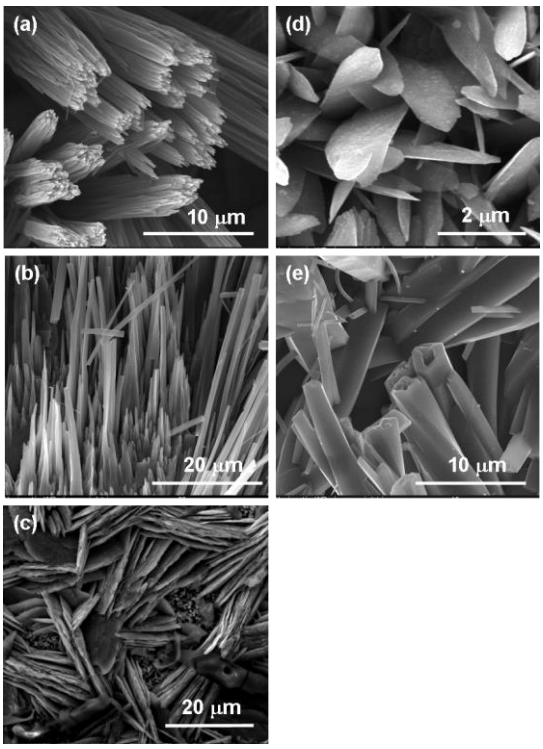

Figure 1: SEM images of (a) CuTCNQ phase I, (b) AgTCNQ (c) CuTCNQ phase II, (d) $CuTCNQF_4$, and (e) $AgTCNQF_4$.

The chemical nature of all materials was characterised by FT-IR, Raman and XRD analysis and correlated with previously reported chemical and structural characterisation studies. Briefly FT-IR spectroscopy gave signature bands for each material which are listed in Table S1 in the supporting information. The main peaks associated with CuTCNQ phase I are at 2206, 2172 (ν(C≡N) region) which are lower than that of neutral TCNQ at 2221 cm^{-1} indicating that TCNQ is in the reduced form. IR bands at 1509 cm^{-1} (ν(C=C) region) and 823 cm^{-1} (ν(C-H) region) also support the presence of reduced TCNQ.[13, 17] For phase II CuTCNQ a characteristic band at 2210 cm^{-1} was observed.[13] For AgTCNQ IR bands consistent with the formation of reduced TCNQ were also observed[12, 30] (Table S1). Raman spectroscopy has proved to be extremely useful in fingerprinting MTCNQ materials. This is due to the significant shift to lower wavenumbers in the C-CN wing stretching mode at 1449 cm^{-1} and C-N stretching mode at 2222 cm^{-1} for neutral TCNQ to 1378 and 2205 cm^{-1} for CuTCNQ and 1384 and 2209 cm^{-1} for AgTCNQ (as seen in Figure 2a) which again indicates that TCNQ is in the reduced form.[30] For the fluorinated analogues the FT-IR spectra demonstrated typical (ν(C=C) bands at a higher energy of 1502 cm^{-1} for $CuTCNQF_4$ and 1497 cm^{-1} for

$AgTCNQF_4$ compared to neutral TCNQ at 1493 cm^{-1} which is highly indicative of $TCNQF_4$ being in the reduced form[24] (Table S1). The Raman spectrum for neutral $TCNQF_4$ consists of bands at 2223, 1662 and 1452 cm^{-1} which correspond to C≡N, C=C ring and C-CN wing stretching modes respectively. A lower Raman shift for the C=C ring and C-CN wing stretching modes for $CuTCNQF_4$ and $AgTCNQF_4$ as a consequence of $TCNQF_4$ being in a reduced form is observed (Figure 2b and Table S1).[24] To confirm the purity and crystal structure of these materials XRD analysis was carried out and shown in Figure S2. The XRD patterns are consistent with previous structural studies.

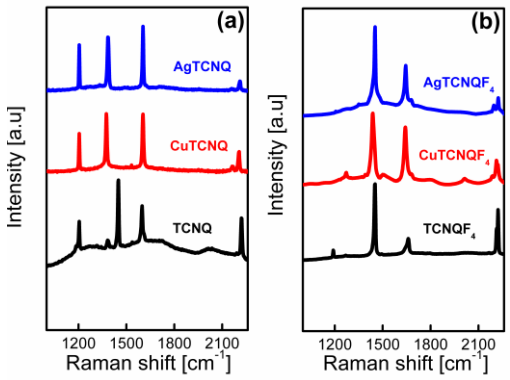

Figure 2: Raman spectra of (a) TCNQ, CuTCNQ and AgTCNQ and (b) $TCNQF_4$, $CuTCNQF_4$ and $AgTCNQF_4$.

As mentioned previously materials of this type have been limited in their application and therefore they were explored for their capability in catalysing electron transfer reactions. An added advantage of using surfaces rather than colloidal nanoparticles is that detrimental effects on performance such as aggregation and recovery of the catalyst and its re-use are avoided. The well known model system of potassium ferricyanide reduction by sodium thiosulphate was chosen to illustrate the activity of these materials and their potential use as heterogeneous liquid phase catalysts. Significantly this reaction has almost exclusively been limited to colloidal coinage metals as the catalyst. The reaction of interest can be written as

$$2[Fe(CN)_6]^{3-} + 2S_2O_3^{2-} \rightarrow 2[Fe(CN)_6]^{4-} + S_4O_6^{2-} \qquad (1)$$

and conveniently monitored by UV-visible spectroscopy through monitoring changes in the intensity of the peak at ca. 420 nm during the course of the reaction. Illustrated in Figure 3 are time dependent UV-vis spectra recorded for the reduction of 1 mM $[Fe(CN)_6]^{3-}$ using 0.1

M $S_2O_3^{2-}$ in the presence of a film of AgTCNQ (Figure 3a) and $AgTCNQF_4$ grown on silver foil of equal area (0.158 cm^2) (Figure 3b).

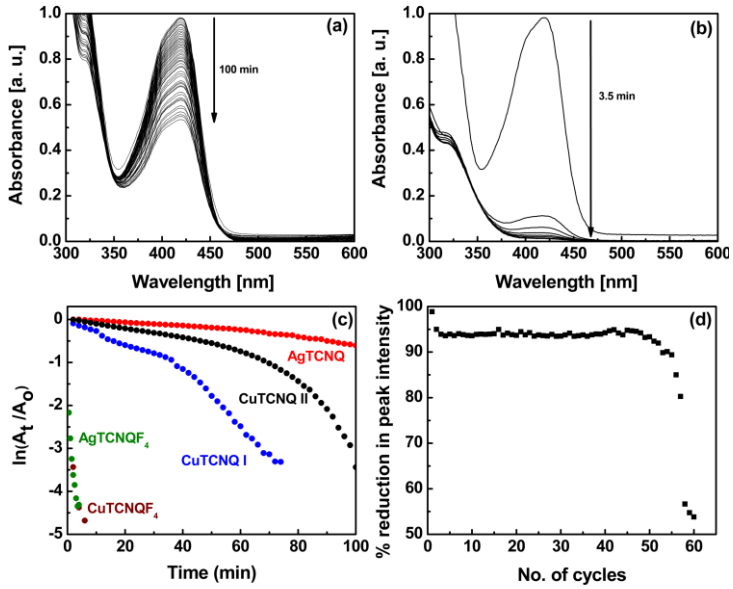

Figure 3: Time dependent UV-vis spectra recorded for the reduction of 1 mM of $Fe(CN)_6^{3-}$ with 0.1 M $S_2O_3^{2-}$ in a total volume of 30 mL catalysed by (a) AgTCNQ (b) $AgTCNQF_4$ (c) plot of $\ln(A_t/A_0)$ versus time for AgTCNQ, $AgTCNQF_4$, CuTCNQ phase I and II and $CuTCNQF_4$ (d) percentage conversion of $[Fe(CN)_6]^{3-}$ to $[Fe(CN)_6]^{4-}$ for separate catalytic runs carried out in a 3 ml volume using $AgTCNQF_4$.

It is immediately apparent that the introduction of AgTCNQ results in a gradual decrease in the intensity of the peak at 420 nm (Figure 3a), however using $AgTCNQF_4$ results in a significant increase in the rate of reduction (Figure 3b). The kinetics of this reaction can be determined by plotting $\ln(A_t/A_0)$ vs Time (Figure 3c) and taking the slope of the linear part of the graph, where A_t is the intensity of the absorbance peak at time t and A_0 is the peak intensity at time zero. The reaction is also assumed to be first order as an excess of $S_2O_3^{2-}$ is used. Interestingly the rate increases from 5.8 x 10^{-3} min^{-1} to 0.61 min^{-1} upon simply employing the fluorinated analogue of AgTCNQ. Significantly this effect was also observed in the case of $CuTCNQF_4$ where an enhanced rate (0.31 min^{-1}) compared to both CuTCNQ phase I and phase II was observed (Figure 3c). The rates of reaction obtained at $CuTCNQF_4$ and $AgTCNQF_4$ are higher compared to many solution dispersed noble metal catalysts (2.54 x 10^{-3} min^{-1} at Pt nanoparticles[31]). It should be noted that these are apparent rate constants

and as pointed out by Jana[32] will be dependent on reaction conditions. In this case the amount of catalyst used is higher than solution dispersed Pt nanomaterials. However, for a surface confined catalyst layer the rate of the reaction is higher than the recently reported gold nanoparticle doped mesoporous boehmite films[32] (3.12×10^{-3} min^{-1}) which used an overall sample area of 1 cm^2 compared to 0.158 cm^2 used in this study. This type of performance is also noteworthy as the reaction is carried out in a total volume of 30 mL which is significantly larger than that usually reported for the coinage metals where solution volumes typical of a UV-vis cuvette of 3 mL are used.

The reusability of the most active material, namely $AgTCNQF_4$, was then tested in a reduced volume of 3 mL containing 1 mM ferricyanide and 0.1 M thiosulphate. The $AgTCNQF_4$ sample was immersed for one minute under stirring conditions after which a UV-vis spectrum was recorded. This was repeated multiple times in fresh 3 mL solutions where the sample was washed with MilliQ water between runs. Figure 3(d) shows the percentage reduction in the intensity of the peak at 420 nm due to $[Fe(CN)_6]^{3-}$ ions for each experiment. A 95% reduction in peak intensity was maintained for 50 runs after which a gradual decrease in activity was observed. However even after 60 runs a 50% intensity reduction was still achieved. Raman and FT-IR spectroscopy recorded after catalytic testing did not show any degradation in the chemical composition of $AgTCNQF_4$ and only minor shifts in the principal peaks were observed (Table S2 and S3). It should be noted that the morphology did change to an extent where some restructuring of the individual rods became evident (Figure S3). However dissolution of the material is discounted as characteristic peaks for $TCNQF_4^{-}{}_{(aq)}$ were not observed in the UV-vis spectrum in the 600-800 nm region (Figure S4).[33] This also excludes the possibility of a homogeneous catalytic reaction occurring between dissolved $AgTCNQF_4$ and $[Fe(CN)_6]^{3-}$.

Generally it is regarded that catalytic reactions are promoted at highly nanostructured materials. Therefore it is unlikely that the increased reaction rate observed here for $MTCNQF_4$ materials is due to a morphological effect as the more active $AgTCNQF_4$ crystallised as large columnar rods of ca. 2 – 5 μm diameter (Figure 2e) compared to the thin high aspect ratio AgTCNQ needles with a width of < 1 μm (Figure 2b). It is known that the bulk conductivity of the fluorinated analogues is significantly less than that of the MTCNQ based materials[34] which suggests that lateral charge propagation through the bulk of the film to maintain the reaction also does not play a role. To test this hypothesis further CuTCNQ phase II was prepared and its catalytic activity was inherently better than AgTCNQ (Figure

3c) even though their bulk conductivities are reported to be comparable with values of 1.3 x 10^{-5} and 1.25 x 10^{-6} S cm^{-1} for CuTCNQ phase II and AgTCNQ respectively.[14] It is also interesting to note that the rate of reaction for both phase I (conductivity = 0.2 S cm^{-1})[13] and phase II CuTCNQ are comparable after ca. 80 min reaction time (Figure 3c). Taking the slope of the linear part of the plot for CuTCNQ phase II (80 to 100 min) gives a rate constant of 7.6 x 10^{-2} min^{-1} compared to 6.7 x 10^{-2} min^{-1} for phase I (40 to 80 min). Interestingly, the crystal structure of $AgTCNQF_4$ is analogous to that of CuTCNQ phase II in that both materials contain interpenetrating TCNQ networks where the neighbouring TCNQ stacks are rotated by around 90°.[12] This similarity in structure is also responsible for their lower bulk conductivity compared to phase I CuTCNQ which has efficient π-stacking between the interpenentrating TCNQ networks. Therefore, the crystalline structure of the materials appears not to play a significant role in the catalytic activity due to the large difference in rate measured for phase II CuTCNQ and $AgTCNQF_4$. The wetability of the surface may also play a role but our recent results in this area for highly porous MTCNQ materials demonstrated that non porous CuTCNQ and $CuTCNQF_4$ materials had comparable water contact angles.[25] A further control experiment was also carried out in the dark and analogous results were achieved which eliminates any possible photocatalytic effect. The possibility of re-oxidation of ferrocyanide by dissolved oxygen is discounted as this reaction only becomes significant at higher temperatures (> 433 K) and an oxygen partial pressure of 2 MPa,[35] which was confirmed experimentally under room temperature conditions where a comparable rate constant for ferricyanide reduction was achieved for CuTCNQ phase I (data not shown). Therefore the enhanced performance at the fluorinated materials is likely to be governed by charge injection/ejection processes into and out of the surface of the individual semi-conducting MTCNQ and $MTCNQF_4$ crystals.

To gain further insight into this effect and what is happening at the surface of these materials during the course of this reaction, open circuit potential (OCP) versus time experiments were carried out which are highly sensitive to the solid solution interface and have been used to monitor processes such as self assembled monolayer formation[36] and diazonium salt grafting at electrode surfaces,[37] galvanic replacement reactions[38] and surface adsorption.[39] In particular this method is useful in determining the accumulation and/or dissipation of surface charge. 1 mM $[Fe(CN)_6]^{3-}$ was initially present in the electrochemical cell and stirred for a period of 600 s while the OCP vs Time was recorded. This was sufficient time to establish a steady OCP value at the surface (Figure 4a-d). At this time the

required volume of $S_2O_3^{2-}$ was injected into the cell (indicated by the arrow in Figure 4a-d) to give a final concentration of 0.1 M and the OCP vs Time profile was continuously monitored. It is clear that the OCP decreases in all cases once thiosulphate is injected into the solution. This is indicative of a process that either decreases positive charge or increases negative charge on the surface.[36] For the system under study here the latter occurs which was confirmed by performing experiments in a solution of 0.1 M $S_2O_3^{2-}$ only which show that the OCP is significantly lower than in the presence of $[Fe(CN)_6]^{3-}$ only (red curves in Figure 4a-d). From the UV-vis results the catalytic reaction is significantly faster for the fluorinated materials. The end of the reaction is indicated by the asterisk in Figure 4a-d where it can be seen in the presented time frame that the reaction at both AgTCNQ and CuTCNQ is not completed. Indeed for $AgTCNQF_4$ the reaction is over in the time frame where a pseudo steady state potential is maintained at the surface of $AgTCNQF_4$ in the presence of $S_2O_3^{2-}$ only. For the silver based materials it suggests that the accumulation of negative charge at the surface via electron injection from thiosulphate is not the limiting step given that comparable OCP values were attained over the first 1200 s of reaction. Once the reaction is completed at $AgTCNQF_4$ the OCP continues to decrease in a manner similar to that observed in $S_2O_3^{2-}$ only.

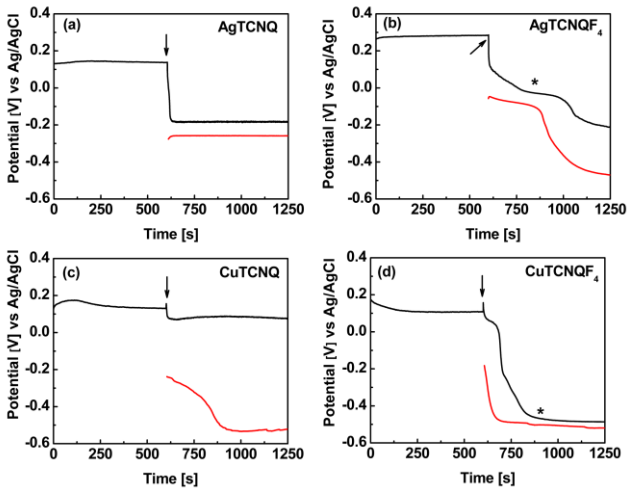

Figure 4: OCP vs Time recorded in a 30 mL solution containing 1 mM $[Fe(CN)_6]^{3-}$ after which $S_2O_3^{2-}$ (0.1 M) was added after 600 s (–) indicated by an arrow and 0.1 M $S_2O_3^{2-}$ only (–) (note data has been translated horizontally to coincide with the injection point for the catalytic run), at (a) AgTCNQ, (b) $AgTCNQF_4$ (c) CuTCNQ phase I and (d) $CuTCNQF_4$.

In the case of the copper based materials a difference was observed in the OCP versus Time data compared to the silver case where the accumulation of negative charge at CuTCNQ was significantly less than that observed for $CuTCNQF_4$ and suggests in this case that it may indeed play a factor in the large catalytic activity difference. For the reaction to proceed electrons must also be transferred to the ferricyanide ions at the catalyst surface and therefore to probe this half of the reaction electrochemical impedance spectroscopy (EIS) was used to determine the resistance to charge transfer at the interface which may be controlling the reaction. The experiment was performed at the open circuit potential in a solution containing 5 mM $[Fe(CN)_6]^{3-/4-}$ and is shown in Figure 5.

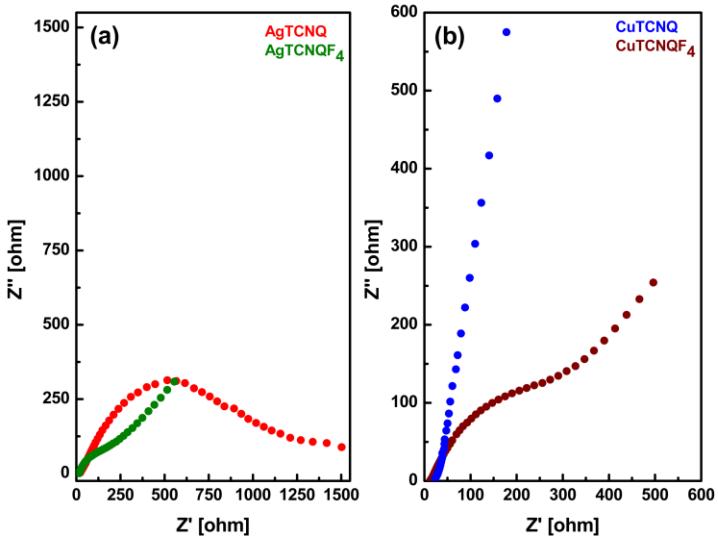

Figure 5: Nyquist plots obtained in 5 mM $[Fe(CN)_6]^{3-/4-}$ and 0.1 M NaCl at OCP for (a) AgTCNQ (–), $AgTCNQF_4$(–) and (b) CuTCNQ phase I (–) and $CuTCNQF_4$ (–).

For $AgTCNQF_4$ the Nyquist plots show that the semi circle component at intermediate frequencies is significantly less compared to AgTCNQ which shows an extremely broad response. The semicircle portion at higher frequencies corresponds to the electron transfer kinetics of the redox species at the electrode surface, while at lower frequencies a linear response is observed that corresponds to diffusion limited electron transfer. Therefore this suggests less resistance to charge transfer at the solid solution interface[40] which would explain the increased rate of reaction. However for CuTCNQ it can be seen that the resistance to charge transfer is significantly less than that recorded for $CuTCNQF_4$ as evidenced by the decrease in width of the semicircle component. This implies that in the copper case it is the injection of charge into the material which limits the reaction rate and not the transfer of electrons to the ferricyanide ions. This was further confirmed by running EIS experiments in

0.1 M $S_2O_3^{2-}$ only where the resistance to charge transfer from $S_2O_3^{2-}$ to $CuTCNQF_4$ was significantly lower than the case for CuTCNQ (Figure S5) as suggested by the OCP versus Time data. Therefore it appears that there needs to be a balance between charge injection into the semiconducting material and ejection from the surface to facilitate the catalytic reaction. In this particular work it can be seen that $AgTCNQF_4$ is the best material for attaining this balance. The exact origin of why this is achieved will require further investigation, however the greater degree of charge transfer from the metal to $TCNQF_4$ compared to TCNQ may be an important aspect as it is known to influence the work function of a material. The fluorinated materials have been reported to have lower work functions than non-fluorinated TCNQ,[41] which will influence charge injection and electron transfer at the solid-solution interface as often encountered in electrochemical experiments carried out with redox active species at conventional semiconductors.

4. Conclusions

In summary, the fabrication of both MTCNQ and $MTCNQF_4$ (M = Cu, Ag) surfaces can be achieved through a redox reaction between the relevant metal surface and an acetonitrile solution containing TCNQ or $TCNQF_4$. Interestingly the catalytic reduction of ferricyanide with thiosulphate on the fluorinated materials is significantly enhanced compared to the TCNQ based materials even though their bulk conductivity is markedly lower. This suggests that lateral charge propagation though the sample is not limiting the process. The morphology and chemical structure of the materials also does not seem to play a dominant role and it was found that a balance needs to be achieved between the accumulation of negative charge at the surface once thiosulphate is introduced into the solution and its transfer to the ferricyanide ions which is most effective at $AgTCNQF_4$. The catalytic activity of $AgTCNQF_4$ was found to be the highest and importantly maintained this activity for up to 50 cycles. Also because these catalysts are confined to a surface the problems associated with solution dispersed metal nanoparticles such as aggregation, separation from the reaction solution and their re-use are alleviated and may therefore have many practical uses for other important reactions.

Acknowledgements

AOM gratefully acknowledges the award of a Future Fellowship from the Australian Research Council (FT110100760). The authors acknowledge the facilities and technical

assistance of the Australian Microscopy & Microanalysis Research Facility at the RMIT Microscopy & Microanalysis Facility.

Notes and references

[a]*School of Applied Sciences, RMIT University, GPO Box 2476V, Melbourne VIC 3001 Australia; E-mail: anthony.omullane@rmit.edu.au*

[b]*Centre for Advanced Materials and Industrial Chemistry,* [a]*School of Applied Sciences, RMIT University, GPO Box 2476V, Melbourne VIC 3001 Australia.*

† Electronic Supplementary Information (ESI) available: Low magnification SEM images of CuTCNQ, AgTCNQ, $CuTCNQF_4$ and $AgTCNQF_4$. FT-IR and Raman data for all catalysts before and after reaction, XRD data of all materials, SEM images of $AgTCNQF_4$ after catalytic reaction and time dependent UV-vis spectra recorded during the catalytic reaction at $AgTCNQF_4$ over an extended wavelength region.

[1] R. S. Potember, T. O. Poehler, D. O. Cowan, A. N. Bloch, *NATO ASI Ser., Ser. C:*, 1980, **56**, 419-428.

[2] Y. Liu, L. Jiang, H. Dong, Z. Tang, W. Hu, *Small*, 2011, **7**, 1412-1415.

[3] R. Müller, O. Rouault, A. Katzenmeyer, L. Goux, D. J. Wouters, J. Genoe, P. Heremans, *Phil. Trans. A*, 2009, **367**, 4191-4201.

[4] B. Mukherjee, M. Mukherjee, J.-e. Park, S. Pyo, *J. Phys. Chem. C*, 2009, **114**, 567-571.

[5] H. Liu, Z. Liu, X. Qian, Y. Guo, S. Cui, L. Sun, Y. Song, Y. Li, D. Zhu, *Crystal Growth & Design*, 2009, **10**, 237-243.

[6] H. Liu, S. Cui, Y. Guo, Y. Li, C. Huang, Z. Zuo, X. Yin, Y. Song, D. Zhu, *J. Mater. Chem.*, 2009, **19**, 1031-1036.

[7] R. Muller, J. Genoe, P. Heremans, *Appl. Phys. Lett.*, 2006, **88**.

[8] R. Muller, S. De Jonge, K. Myny, D. J. Wouters, J. Genoe, P. Heremans, *Solid-State Electronics*, 2006, **50**, 602-606.

[9] H. Liu, Q. Zhao, Y. Li, Y. Liu, F. Lu, J. Zhuang, S. Wang, L. Jiang, D. Zhu, D. Yu, L. Chi, *J. Am. Chem. Soc.*, 2005, **127**, 1120-1121.

[10] T. Oyamada, H. Tanaka, K. Matsushige, H. Sasabe, C. Adachi, *Appl. Phys. Lett.*, 2003, **83**, 1252-1254.

[11] K. Xiao, I. N. Ivanov, A. A. Puretzky, Z. Liu, D. B. Geohegan, *Adv. Mater.*, 2006, **18**, 2184-2188.

[12] S. A. O'Kane, R. Clerac, H. Zhao, X. Ouyang, J. R. Galan-Mascaros, R. Heintz, K. R. Dunbar, *J. Solid State Chem.*, 2000, **152**, 159-173.

[13] R. A. Heintz, H. Zhao, X. Ouyang, G. Grandinetti, J. Cowen, K. R. Dunbar, *Inorg. Chem.*, 1999, **38**, 144-156.

[14] A. R. Harris, A. Nafady, A. P. O'Mullane, A. M. Bond, *Chem. Mater.*, 2007, **19**, 5499-5509.

[15] A. P. O'Mullane, A. K. Neufeld, A. R. Harris, A. M. Bond, *Langmuir*, 2006, **22**, 10499-10505.

[16] A. R. Harris, A. K. Neufeld, A. P. O'Mullane, A. M. Bond, R. J. S. Morrison, *J. Electrochem. Soc.*, 2005, **152**, C577-C583.

[17] A. K. Neufeld, I. Madsen, A. M. Bond, C. F. Hogan, *Chem. Mater.*, 2003, **15**, 3573-3585.

[18] C. Zhao, A. M. Bond, *J. Am. Chem. Soc.*, 2009, **131**, 4279-4287.

[19] A. P. O'Mullane, N. Fay, A. Nafady, A. M. Bond, *J. Am. Chem. Soc.*, 2007, **129**, 2066-2073.

[20] K. Xiao, A. J. Rondinone, A. A. Puretzky, I. N. Ivanov, S. T. Retterer, D. B. Geohegan, *Chem. Mater.*, 2009, **21**, 4275-4281.

[21] S. Cui, Y. Li, Y. Guo, H. Liu, Y. Song, J. Xu, J. Lv, M. Zhu, D. Zhu, *Adv. Mater.*, 2008, **20**, 309-313.

[22] C. Ouyang, Y. Guo, H. Liu, Y. Zhao, G. Li, Y. Li, Y. Song, Y. Li, *J. Phys. Chem. C*, 2009, **113**, 7044-7051.

[23] K. Xiao, M. Yoon, A. J. Rondinone, E. A. Payzant, D. B. Geohegan, *J. Am. Chem. Soc.*, 2012, **134**, 14353-14361.

[24] T. Le, A. O'Mullane, L. Martin, A. Bond, *J. Solid State Electrochem.*, 2011, **15**, 2293-2304.

[25] M. Mahajan, S. K. Bhargava, A. P. O'Mullane, *Electrochim. Acta*, 2012, doi: 10.1016/j.electacta.2012.1009.1068.

[26] C.-a. Di, G. Yu, Y. Liu, Y. Guo, W. Wu, D. Wei, D. Zhu, *Phys. Chem. Chem. Phys.*, 2008, **10**, 2302-2307.

[27] A. Pearson, A. P. O'Mullane, V. Bansal, S. K. Bhargava, *Inorg. Chem.*, 2011, **50**, 1705-1712.